

A SPECTROSCOPIC STUDY OF FIELD AND RUNAWAY OB STARS

M. VIRGINIA MCSWAIN^{1,2}

Department of Astronomy, Yale University, New Haven, CT; mcswain@astro.yale.edu

AND

TABETHA S. BOYAJIAN,¹ ERIKA D. GRUNDSTROM,¹ AND DOUGLAS R. GIES

Department of Physics and Astronomy, Georgia State University, Atlanta, GA;

tabetha@chara.gsu.edu, erika@chara.gsu.edu, gies@chara.gsu.edu

Received 2006 August 12; accepted 2006 October 3

ABSTRACT

Identifying binaries among runaway O- and B-type stars offers valuable insight into the evolution of open clusters and close binary stars. Here we present a spectroscopic investigation of 12 known or suspected binaries among field and runaway OB stars. We find new orbital solutions for five single-lined spectroscopic binaries (HD 1976, HD 14633, HD 15137, HD 37737, and HD 52533), and we classify two stars thought to be binaries (HD 30614 and HD 188001) as single stars. In addition, we reinvestigate their runaway status using our new radial velocity data with the UCAC2 proper-motion catalogs. Seven stars in our study appear to have been ejected from their birthplaces, and at least three of these runaways are spectroscopic binaries and are of great interest for future study.

Subject headings: binaries: spectroscopic — stars: early-type — stars: individual (Feige 25, HD 1976, HD 14633, HD 15137, HD 30614, HD 36576, HD 37737, HD 52266, HD 52533, HD 60848, HD 188001, HD 195592) — stars: kinematics

1. INTRODUCTION

Nearly all O- and B-type stars are believed to form in open clusters and stellar associations, but a handful of OB stars are observed at high Galactic latitudes and with large peculiar space velocities, suggesting that they have been ejected from the cluster of their birth. There are two accepted mechanisms to explain the origin of these runaway O- and B-type stars. In one scenario, close multibody interactions in a dense cluster environment cause one or more stars to be scattered out of the region (Poveda et al. 1967). In rare cases, the ejected stars may be bound as a binary pair; Leonard & Duncan (1990) used *N*-body simulations of open clusters to show that a binary frequency of about 10% is expected from dynamical ejections. An alternative mechanism involves a supernova explosion within a close binary, ejecting the secondary due to the conservation of momentum (Zwicky 1957; Blaauw 1961). The resulting neutron star may remain bound to the secondary if not enough mass is lost during the explosion. Portegies Zwart (2000) predicted a binary fraction of 20%–40% among runaways that are ejected by such a binary supernova scenario. The observed fraction of binaries among runaways seems consistent with either scenario (5%–26%; Mason et al. 1998).

Observational evidence suggests that both dynamical interactions and supernovae in close binaries do produce some runaway systems. The microquasar LS 5039 was likely ejected from the Milky Way disk about 1.1 Myr ago by the supernova explosion of the neutron star progenitor (Ribó et al. 2002; McSwain et al. 2004; Casares et al. 2005). Berger & Gies (2001) found that about 7% of Be stars have high peculiar space velocities, likely due to energy received during the supernova of a close binary companion (McSwain & Gies 2005). On the other hand, Gualandris

et al. (2004) showed that a four-body encounter 2.5 Myr ago in the Trapezium cluster resulted in three ejected systems: two single stars and one binary. The single stars both have very large space velocities and are classified as runaways, although the ejected binary has a lower space velocity due to its higher total mass. In a study of 44 Trapezium-type clusters, Allen et al. (2006) found four stars with large transverse velocities that were likely ejected by dynamical interactions.

Which process dominates the production of runaway stars? Hoogerwerf et al. (2001) showed that massive runaways tend to have enriched helium abundances and higher rotational velocities, while fewer nonrunaways exhibit these traits. While rotational mixing could explain these results, it is doubtful that mixing occurs preferentially among runaways. It is more likely that prior mass transfer of CNO-processed material from the evolved donors has altered the surface abundances and added angular momentum to the mass gainers. The high binding energy of close massive binaries makes it unlikely that they will be disrupted by dynamical interactions, but they could be separated by a supernova. Thus, according to Hoogerwerf et al. (2001) the evidence favors the supernova ejection scenario over dynamical cluster interactions. However, pulsar searches by Philp et al. (1996) and Sayer et al. (1996) have not identified any neutron stars among runaway OB stars, and further investigation of their properties is needed.

The production of runaway OB binaries is expected to be rare, but these systems can offer key insights into the evolution of close binary stars and open clusters. If massive stars form in dense regions through the mergers of low-mass protostellar cores, the expected multibody interactions will result in a large number of high-velocity runaways (Bally & Zinnecker 2005). Ejecting a star dynamically from a young cluster will reduce the total energy imparted to the cluster via stellar winds, radiation, and supernova ejecta, whereas a protosupernova system will remain in the cluster for a longer time and contribute more energy into its environment (Dray et al. 2005). Finally, the relative importance of the supernova ejection scenario places limits on the mass needed to form black holes and neutron stars (Dray et al. 2005).

¹ Visiting Astronomer, Kitt Peak National Observatory, National Optical Astronomy Observatory, operated by the Association of Universities for Research in Astronomy, Inc., under contract with the National Science Foundation (NSF).

² NSF Astronomy and Astrophysics Postdoctoral Fellow.

In this work, we examine the binary status of 12 field and runaway OB stars. Through a radial velocity study of these stars, we determine the orbital solutions of five single-lined spectroscopic binaries (SB1s). One is a possible triple star, and we also find two suspected SB1 systems. By fitting the spectral energy distributions of these stars, we measure their reddening and angular sizes to constrain their distances. Finally, our radial velocities combined with proper motions allow us to measure their peculiar space velocities and reinvestigate the runaway status of these targets. Our results reveal that only seven of the 12 stars have high space velocities, while five stars may not be runaways. Of the runaways, two are SB1s, and a third is a suspected SB1. We will investigate their cluster ejection scenarios in a forthcoming paper.

2. TARGET SELECTION

Most of our target stars (HD 14633, HD 15137, HD 30614, HD 37737, HD 52266, HD 52533, HD 60848, HD 188001, and HD 195592) have been classified as field or runaway stars by Gies & Bolton (1986), Mason et al. (1998), and/or Stickland & Lloyd (2001). Five of these (HD 30614, HD 52266, HD 60848, HD 188001, and HD 195592) have unknown multiplicity or are suspected SB1s. The others are known SB1 systems. Of this set, HD 14633 and HD 15137 are of particular interest, since both SB1 systems were likely ejected from the open cluster NGC 654, and their travel times appear longer than the expected O star lifetimes (Boyajian et al. 2005). On the other hand, the field stars HD 52266, HD 52533, and HD 195592 may be the dominant members of previously undetected clusters (de Wit et al. 2004).

HD 1976 has been classified as a member of the Cas-Tau OB association (De Zeeuw et al. 1999) and is a visual binary (Docobo & Costa 1986). It is also a slowly pulsating B star (Mathias et al. 2001) and a known SB1 (Blaauw & van Albada 1963). Although it is not a field star or a runaway, we include it in our observational program because its poorly known orbital solution (Blaauw & van Albada 1963; Abt et al. 1990) indicates a moderate eccentricity and a low-mass function. Refining its orbit could help determine if this system is a postsupernova system whose kick velocity was too small to eject it from the association.

The star HD 36576 is a field Be star (Zorec et al. 2005) and a radial velocity variable (Gies & Bolton 1986). While Gies & Bolton (1986) classified this star as a nonrunaway, Berger & Gies (2001) did not include this star in their sample when they performed a new investigation of high-velocity Be stars using *Hipparcos* proper motions. Therefore, we reinvestigate its runaway status here.

Feige 25 (HIP 12320) is a B-type star at high Galactic latitude (-48.36°) whose abundances and kinematics are consistent with a runaway Population I star (Martin 2004, 2006). Its radial velocity has been measured only twice before by Martin (2006) and Greenstein & Sargent (1974), and those measurements differ by nearly 30 km s^{-1} . Therefore, we suspect that it may be an SB1 system, and we include it here for further investigation.

Most of the selected candidates are not known X-ray emitters, although three (HD 30614, HD 52533, and HD 188001) are known weak X-ray sources. Meurs et al. (2005) showed that the observed X-ray luminosities and hardness ratios of HD 30614 and HD 188001 are consistent with the emission of normal O supergiant stars rather than from X-ray binaries. The hardness ratios of HD 52533 (Voges et al. 2000) are likewise consistent with an origin in a normal O star (Motch et al. 1998). However, Meurs et al. (2005) pointed out that these results do not rule out the presence of a compact companion. If the accretion rate is sufficiently low, the resulting X-ray production may not contribute significantly to the total X-ray luminosity. A deeper X-ray observation may be

able to detect the characteristic hard spectrum of a massive X-ray binary (MXRB) in these systems.

Likewise, none of our targets contain a known pulsar. Philp et al. (1996) searched for pulsars in 44 OB runaway stars, including our targets HD 30614, HD 37737, and HD 52533. Similarly, Sayer et al. (1996) searched for pulsars in HD 14633, HD 36576, and 38 other OB runaways. Although neither group found any pulsars associated with these stars, their existence cannot be ruled out. Using binary population synthesis calculations, Portegies Zwart (2000) found that 20%–40% of OB runaways may have neutron star companions. However, due to the short lifetime of the pulsar (assumed to be 10 Myr) and the absorption of the radio emission by the stellar winds (greater at periastron than apastron), Portegies Zwart (2000) predicted that only 1%–2% of these neutron stars could be visible as radio pulsars at some time during their orbit.

3. OBSERVATIONS AND RADIAL VELOCITIES

Each target was observed during two observing campaigns at the Kitt Peak National Observatory (KPNO) 2.1 m telescope during 2005 October and November. We used the No. 47 grating (831 grooves mm^{-1}) in second order to obtain a resolving power $R = \lambda/\delta\lambda \sim 3000$. The observed wavelength range was 4050–4950 Å, a region that includes numerous H Balmer, He I, and He II lines in O- and B-type stars. The data were reduced using standard routines in IRAF.

We also obtained some spectra from the KPNO 0.9 m coude feed telescope in 2005 November. The resolving power is $R \sim 12,000$ using the long collimator, grating A (in second order with order sorting filter 4-96), camera 5, and the T2KB CCD, a 2048 × 2048 device. We obtained a spectral coverage of 4240–4580 Å.

We used all available strong, unblended lines to measure radial velocities, V_r , in these stars. Rest wavelengths for each line were taken from the National Institute of Standards and Technology (NIST) Atomic Spectra Database.³ We selected one spectrum with good signal-to-noise ratio (S/N) to serve as a template, and we fit the core of each absorption line with a parabola to determine its absolute radial velocity. The remaining spectra were then cross-correlated with this template to determine the relative velocities. Several lines in the 2.1 m data sets lie near bad pixels that corrupted the cross correlations, so these lines were usually omitted. In a few cases we found systematic differences between sets of lines, and we discuss these below. Only in the case of HD 1976, we found a systematic disagreement between our measurements and those in the literature. Our V_r measurements of all other stars were in good agreement with previous measurements. For each star, we list the complete set of lines used in Table 1, and the resulting mean velocities are listed in Tables 4 and 5. For the stars in Table 5, we also include the standard deviation, σ , of the V_r measured from many lines for each observation.

To test the significance of systematic night-to-night (NN) and line-to-line (LL) variations, we performed a two-way analysis of variance (2AOV) statistical test for each set of velocities. This test is described in detail by Gies & Bolton (1986). Essentially, it allows us to test the null hypothesis that the star does not exhibit statistically significant variations. The F -statistic describes the variance of the entire data set divided by the average variance of each measurement, and p gives the probability that the observed variations are drawn from the same random distribution. If p is small, less than 1%, then we must reject the null hypothesis. Thus, a low p indicates that the observed differences in V_r are significant.

³ The NIST Atomic Spectra Database is available online at <http://physics.nist.gov/PhysRefData/ASD/index.html>.

TABLE 1
LINES USED FOR RADIAL VELOCITIES

Star	Telescope	Lines
HD 1976	2.1 m coudé	H β , H γ , H δ , He I $\lambda\lambda$ 4144, 4388, 4471, 4713, 4922, C II λ 4267, Mg II λ 4481 H γ , He I $\lambda\lambda$ 4388, 4471
HD 14633	2.1 m	H β , H γ , H δ , He I $\lambda\lambda$ 4121, 4144, 4388, 4471, 4713 (Oct only), 4922; He II $\lambda\lambda$ 4200, 4542, 4686; Si IV λ 4116; N III λ 4640 ^a
HD 15137	2.1 m	H β , H γ , H δ , He I $\lambda\lambda$ 4144, 4388, 4471, 4713, 4922; He II $\lambda\lambda$ 4200, 4542, 4686; Si IV λ 4089; N III λ 4379
Feige 25	2.1 m coudé	H β , H γ , H δ , He I $\lambda\lambda$ 4144, 4388, 4471, 4922 (Oct only); Mg II λ 4481 H γ , He I $\lambda\lambda$ 4388, 4471
HD 30614	2.1 m coudé	H β , H γ , H δ , He I $\lambda\lambda$ 4121, 4144, 4388, 4471, 4713, 4921; He II $\lambda\lambda$ 4200, 4542; Si IV $\lambda\lambda$ 4089, 4116; N III λ 4379 H δ , He I $\lambda\lambda$ 4388, 4471; He II λ 4542; N III λ 4379
HD 36576	2.1 m coudé	He I $\lambda\lambda$ 4121, 4144, 4388, 4471, 4713 He I $\lambda\lambda$ 4388, 4471
HD 37737	2.1 m coudé	H β , H γ , H δ , He I $\lambda\lambda$ 4144, 4388, 4471, 4713, 4922; He II $\lambda\lambda$ 4200, 4542, 4686; Si IV λ 4089 H γ , He I $\lambda\lambda$ 4388, 4471; He II λ 4542
HD 52266	2.1 m coudé	H β , H γ , H δ , He I $\lambda\lambda$ 4144, 4388, 4471, 4713, 4921; He II $\lambda\lambda$ 4200, 4542, 4686; Si IV λ 4089 H γ , He I $\lambda\lambda$ 4388, 4471
HD 52533	2.1 m coudé	He II $\lambda\lambda$ 4200, 4542, 4686 He II λ 4542
HD 60848	2.1 m coudé	H δ , He I $\lambda\lambda$ 4144, 4388, 4471, 4921; He II $\lambda\lambda$ 4200, 4542, 4686; Si IV λ 4089; N III λ 4379 He I $\lambda\lambda$ 4388, 4471; He II λ 4542
HD 188001	2.1 m coudé	He I $\lambda\lambda$ 4120, 4144, 4388, 4471, 4713, 4922; He II $\lambda\lambda$ 4200, 4542 He I $\lambda\lambda$ 4388, 4471; He II λ 4542
HD 195592	2.1 m coudé	He I $\lambda\lambda$ 4120, 4143, 4387, 4471, 4713, 4922; He II $\lambda\lambda$ 4200, 4542; Si IV $\lambda\lambda$ 4089, 4116; N III $\lambda\lambda$ 4379, 4640 ^a He I $\lambda\lambda$ 4388, 4471; He II λ 4542

^a Blend.

Both F and p depend on the number of degrees of freedom, which is just the number of input variables (lines or spectra) minus 1.

The coudé feed spectral range is limited and includes only a few of the lines measured in the 2.1 m spectra. Consequently, we applied the 2AOV test to the common line sample in 2.1 m data alone, and these results are summarized in Table 2. The test indicates significant LL variations in HD 1976, HD 15137, HD 30614, HD 37737, HD 52533, and HD 60848. We are not surprised to find LL variations in OB-type stellar spectra because line formation may occur at different levels in an expanding atmosphere and because some lines suffer from blending with weaker nearby components. Furthermore, HD 52533 may have an optical companion causing contamination in its line profiles. Even though these stars do have statistically significant LL variations, we can still identify significant nightly variations in V_r , since we measure a consistent set of lines in the our spectra. Feige 25 and HD 60848 show little evidence of nightly systematic differences, while the nightly variations observed in all other targets are highly significant.

For the stars with significant NN V_r variations, we combined data from the literature (where available) with our own measurements for improved orbital solutions. We performed period searches using a version of the discrete Fourier transform and CLEAN deconvolution algorithm of Roberts et al. (1987) (written in IDL⁴ by A. W. Fullerton). We then tested any significant signal found in the CLEANed power spectrum to verify that it produced a reasonable phased V_r curve. We ruled out periods of less than 1 day because we never observed rapid, high-amplitude changes in V_r among our targets. The best period from the CLEANed power spectrum was used with the nonlinear, least-squares fitting program of Morbey & Brosterhus (1974) to solve for the orbital elements.

A detailed discussion of the results from our radial velocity study is presented below, and we summarize the results here. We were able to improve the known orbital elements for five SB1

⁴ IDL is a registered trademark of Research Systems, Inc.

TABLE 2
RESULTS FROM TWO-WAY ANALYSIS OF VARIANCE TEST

Star	Degrees of Freedom (LL)	F (LL)	p (LL) (%)	Degrees of Freedom (NN)	F (NN)	p (NN) (%)
HD 1976	10	2.54	0.78	13	13.45	0.00
HD 14633	13	1.96	2.72	13	33.65	0.00
HD 15137	12	5.17	0.00	13	3.18	0.03
Feige 25	7	1.43	23.32	4	2.74	4.84
HD 30614	13	11.07	0.00	13	12.17	0.00
HD 36576	4	2.08	9.87	12	8.77	0.00
HD 37737	11	14.39	0.00	12	316.90	0.00
HD 52266	11	1.84	5.22	14	10.38	0.00
HD 52533	9	6.48	0.00	14	13.30	0.00
HD 60848	9	11.35	0.00	13	2.22	1.27
HD 188001	7	1.54	18.09	6	11.36	0.00
HD 195592	11	2.05	3.41	7	7.27	0.00

TABLE 3
ORBITAL ELEMENTS

Star	P (days)	T (HJD-2,400,000)	e	ω (deg)	K_1 (km s ⁻¹)	γ (km s ⁻¹)	$f(m)$ (M_\odot)	$a_1 \sin i$ (R_\odot)	σ (km s ⁻¹)
HD 1976	25.4176 \pm 0.0004	35783.5 \pm 0.1	0.12 \pm 0.03	172 \pm 2	23.6 \pm 0.7	-9.7 \pm 0.5	0.034 \pm 0.003	11.7 \pm 0.4	4.81
HD 14633	15.4082 \pm 0.0004	51885.07 \pm 0.01	0.700 \pm 0.003	138.7 \pm 0.5	19.0 \pm 0.1	-38.17 \pm 0.08	0.0040 \pm 0.0001	4.13 \pm 0.04	1.96
HD 15137	30.35 ^a	51879.7 \pm 0.6	0.48 \pm 0.07	148 \pm 10	13 \pm 1	-48.4 \pm 0.6	0.004 \pm 0.002	6.7 \pm 0.8	3.94
HD 37737	7.8400 \pm 0.0002	53690.2 \pm 0.1	0.43 \pm 0.02	158 \pm 5	72 \pm 2	-8 \pm 2	0.22 \pm 0.02	10.1 \pm 0.3	5.28
HD 52533	22.1861 \pm 0.0002	44635.01 \pm 0.03	0.30 \pm 0.01	330.3 \pm 0.5	105 \pm 1	76.7 \pm 0.6	2.30 \pm 0.07	43.8 \pm 0.4	11.7

^a Fixed.

systems (HD 1976, HD 14633, HD 15137, HD 37737, and HD 52533), and these are listed in Table 3. Their V_r curves are shown in Figure 1, and our V_r measurements are listed in Table 4. The deviations from the theoretical V_r curves are comparable to the errors of the mean.

The stars Feige 25, HD 36576, and HD 60848 appear to be constant-velocity stars. Both HD 36576 and HD 60848 are Be-type objects, so their V_r are affected by variable emission filling the line profiles or photospheric nonradial pulsations changing their line shapes. HD 30614 and HD 188001 have been identified

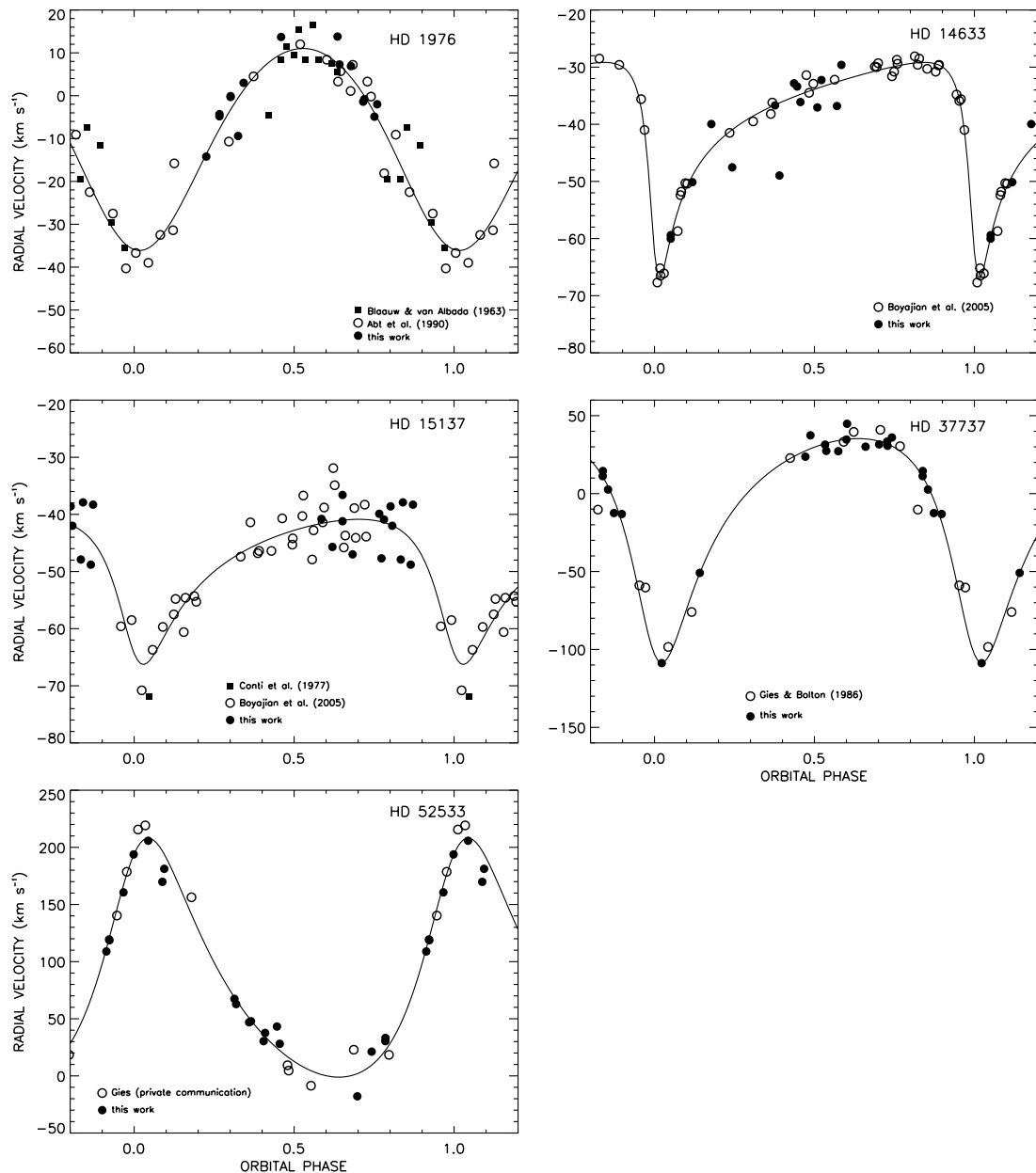


FIG. 1.—Radial velocity curves for binaries with orbital solutions.

TABLE 4
RADIAL VELOCITY MEASUREMENTS OF BINARIES WITH ORBITAL SOLUTIONS

Star	HJD (−2,450,000)	Orbital Phase	V_r (km s ^{−1})	($O-C$) (km s ^{−1})	Star	HJD (−2,450,000)	Orbital Phase	V_r (km s ^{−1})	($O-C$) (km s ^{−1})
HD 1976	3657.787	0.225	−14.2	−0.5	HD 15137	3696.628	0.864	−48.8	−4.4
	3658.833	0.266	−4.8	3.0		3696.841	0.871	−38.3	6.5
	3658.835	0.267	−4.3	3.5	HD 37737	3658.005	0.898	−13.1	5.2
	3659.720	0.301	−0.3	3.0		3658.983	0.023	−108.8	−0.2
	3659.721	0.301	−0.1	3.2		3659.916	0.142	−50.9	0.2
	3660.754	0.342	3.0	1.7		3662.988	0.533	31.4	−0.7
	3663.735	0.459	13.7	4.0		3663.016	0.537	27.4	−4.9
	3685.735 ^a	0.325	−9.4	−8.9		3663.980	0.660	30.1	−5.0
	3693.635	0.636	13.8	6.3		3686.830 ^a	0.575	27.2	−6.7
	3693.790	0.642	7.3	0.2		3687.030 ^a	0.600	34.7	−0.1
	3694.701	0.678	6.9	2.6		3687.832 ^a	0.702	31.6	−2.0
	3695.674	0.716	−1.4	−1.8		3688.037 ^a	0.729	30.7	−1.1
	3695.769	0.720	−0.8	−0.7		3688.900 ^a	0.839	14.5	3.8
	3696.565	0.751	−4.9	−0.9		3689.028 ^a	0.855	2.6	−2.0
	3696.789	0.760	−2.0	3.2		3693.864	0.472	23.7	−3.7
HD 14633	3657.799	0.051	−60.0	−0.2		3693.988	0.488	37.4	8.6
	3657.803	0.051	−59.4	0.3	HD 52533	3694.886	0.602	44.8	9.9
	3658.843	0.118	−50.1	−1.1		3695.868	0.727	33.4	1.5
	3659.756	0.178	−40.0	4.3		3695.985	0.742	36.0	5.5
	3660.760	0.243	−47.5	−6.6		3696.737	0.838	11.2	0.3
	3663.739	0.436	−32.8	2.4		3697.012	0.873	−12.5	−8.6
	3693.639	0.377	−36.7	−0.1		3658.024	0.697	−17.9	−19.8
	3693.852 ^b	0.391	−49.0	−12.7		3659.020	0.742	21.2	11.8
	3694.705	0.446	−33.4	1.6		3659.970	0.785	30.4	8.1
	3694.863	0.456	−36.1	−1.3		3659.978	0.786	33.2	10.8
	3695.679	0.509	−37.1	−3.3		3662.994	0.921	119.4	−0.6
	3695.875	0.522	−32.3	1.2		3663.020	0.923	118.7	−2.5
	3696.624	0.570	−36.8	−4.2		3663.994	0.967	160.6	−6.4
	3696.838	0.584	−29.6	2.7		3684.995 ^{a,c}	0.913	108.9	−2.5
HD 15137	3657.812	0.586	−40.8	0.8		3686.885 ^{a,c}	0.998	193.8	0.6
	3658.850	0.620	−45.7	−4.5		3687.892 ^{a,c}	0.044	205.8	−2.3
	3659.806	0.651	−41.2	−0.2		3688.877 ^{a,c}	0.088	169.8	−27.0
	3659.810	0.651	−36.6	4.4		3689.006 ^{a,c}	0.094	181.2	−12.8
	3660.765	0.683	−47.0	−6.1		3693.875	0.313	67.4	−1.3
	3663.742	0.781	−40.9	0.5		3693.998	0.319	62.8	−3.6
	3693.644	0.766	−39.9	1.3		3694.894	0.359	46.9	−3.7
	3693.855	0.773	−47.7	−6.4		3695.023	0.365	47.8	−0.8
	3694.713	0.801	−38.6	3.2		3695.896	0.404	30.4	−5.4
	3694.876	0.807	−42.0	−0.0		3696.002	0.409	37.6	3.3
	3695.683	0.833	−47.9	−5.1		3696.825	0.446	43.2	18.9
	3695.887	0.840	−37.9	5.2		3697.019	0.455	28.1	5.9

^a Obtained with the coudé feed telescope.

^b Measurement assigned zero weight.

^c Measurement assigned half-weight.

as SB1 systems in the past, but we use available data in the literature to show that they are more likely single stars that have been misclassified. HD 52266 and HD 195592 are likely SB1 systems, but we cannot determine the systems' periods or orbital elements from the available data. The V_r measurements for these stars without orbital solutions in this work are listed in Table 5.

3.1. HD 1976

HD 1976 is a speckle binary with $\delta V = 0.89$ and separation $0.138''$ (Hartkopf et al. 2000; Mason et al. 2001). It is also an SB1, and Blaauw & van Albada (1963) and Abt et al. (1990) each presented orbital solutions for HD 1976. These solutions have somewhat differing orbital periods (27.8 and 25.44 days, respectively) and eccentricity (0.2 and 0.14, respectively).

Unfortunately, our observing schedule did not allow us to obtain good orbital coverage of this system, and we rely heavily on the data of Blaauw & van Albada (1963) and Abt et al. (1990) to determine the period and orbital elements. To update the orbital elements for this SB1, we included our own 15 V_r measurements with those published by Blaauw & van Albada (1963) and Abt et al. (1990) (except four points with large scatter, which we assigned half-weight). We noted a systematic difference between their data and ours, so we added an offset of 4.5 km s^{-1} to the velocities of Blaauw & van Albada (1963) and 5.3 km s^{-1} to the velocities of Abt et al. (1990) to bring our measurements into better agreement. Our period search revealed two possible results, 25.4 or 27.6 days, and we investigated many possible periods close to these values to obtain the lowest errors in the orbital fit. The

TABLE 5
RADIAL VELOCITY MEASUREMENTS OF OTHER STARS

Star	HJD (−2,450,000)	V_r (km s ^{−1})	σ (km s ^{−1})	Star	HJD (−2,450,000)	V_r (km s ^{−1})	σ (km s ^{−1})
Feige 25	3657.834 ^a	34.3	10.4	HD 52266	3663.991	20.5	10.9
	3658.867 ^a	36.0	5.6		3684.985 ^c	30.2	18.4
	3663.749	47.3	11.4		3693.871	39.0	8.2
	3688.815 ^b	25.3	16.3		3693.993	39.2	12.6
	3693.838	39.4	7.1		3694.891	33.7	6.4
	3696.689 ^a	43.3	12.9		3695.019	33.5	5.8
					3695.893	32.7	9.1
HD 30614	3657.989	8.9	12.5		3695.999	29.5	13.9
	3658.906	9.0	6.3		3696.822	31.7	13.4
	3659.010	3.2	6.8		3697.016	38.8	9.4
	3659.899	22.7	10.2	HD 60848	3658.032	13.5	14.1
	3659.901	10.5	8.6		3659.026	20.7	14.9
	3662.980	22.5	7.9		3659.987	18.9	17.8
	3663.976	13.3	16.2		3659.995	26.6	15.0
	3686.859 ^c	2.2	11.4		3663.002	19.7	13.6
	3693.858	2.9	7.4		3663.999	21.4	14.3
	3693.983	1.6	9.7		3685.004 ^c	33.8	15.4
	3694.879	22.7	9.1		3693.879	10.2	12.7
	3695.000	13.3	9.3		3694.001	26.0	16.7
	3695.861	18.4	10.7		3694.897	26.8	14.4
	3695.978	15.4	14.6		3695.026	18.5	13.4
	3696.731	9.8	8.6		3695.898	21.2	7.4
HD 36576	3657.996	62.7	28.8		3696.005	26.1	9.7
	3658.978	37.8	6.7		3696.827	21.9	14.5
	3659.911	21.4	7.2		3697.021	17.5	10.2
	3662.983	44.6	7.7	HD 188001	3657.649	16.9	6.3
	3663.985	35.1	8.2		3661.609	20.8	7.6
	3686.866 ^c	62.1	23.6		3663.570	21.8	8.5
	3687.913 ^c	74.2	39.0		3687.603 ^c	11.8	9.4
	3693.869	23.5	11.4		3693.551	6.3	5.3
	3693.992	27.4	10.1		3694.561	6.2	6.5
	3694.890	45.1	9.5		3695.556	16.0	4.3
	3695.019	55.4	8.7		3696.553	25.3	6.1
	3695.871	58.3	6.7	HD 195592	3657.668	−24.5	12.2
	3695.988	53.9	5.4		3657.671	−23.2	3.9
	3696.741	61.4	7.2		3661.615	−19.3	7.4
	3697.009	34.8	8.9		3663.574	−19.0	7.8
HD 52266	3658.013	14.9	18.5		3688.620 ^c	−20.4	3.2
	3659.013	17.2	6.7		3693.556	−28.7	6.8
	3659.956	15.4	6.7		3694.566	−26.8	5.3
	3659.961	16.5	6.8		3695.561	−32.1	4.8
	3662.998	24.2	7.9		3696.558	−32.8	6.2
	3663.026	12.7	15.1				

^a Obtained using co-added spectra from 2.1 m telescope.

^b Obtained using co-added spectra from coudé feed telescope.

^c Obtained with the coudé feed telescope.

resulting errors were 2 times smaller using the shorter period, and we adopt a period of 25.4176 days. The remaining orbital elements for HD 1976 are listed in Table 3.

We expect that the speckle companion contributes about 30% of the flux in this system, but we saw no signs of blending in the H Balmer or He I line profiles. However, the relatively low velocity semiamplitude, K , and high $v \sin i$ of this star (see § 4) may prevent us from detecting the spectrum of the companion star.

3.2. HD 14633

In our earlier V_r study of HD 14633 (Boyajian et al. 2005), we determined that this SB1 has a short period ($15.4083 \pm$

0.0004 days), high eccentricity, and low-mass function. This system may harbor a compact companion formed by a past supernova, making it one of the first known quiet MXRB candidates. In Table 4, we present 14 new V_r measurements of this system.

To improve the orbital period, we combined a total of 103 V_r measurements from Bolton & Rogers (1978), Stone (1982), Boyajian et al. (2005), and this work. We refine the period to 15.407 days. From the recent data of Boyajian et al. (2005) and this work, we also improved the orbital elements, listed in Table 3. One point at $\phi \sim 0.4$ has a very large scatter, and we assigned it zero weight in the fit. The new orbital elements are the same within errors as our earlier values (Boyajian et al. 2005).

3.3. HD 15137

Likewise, HD 15137 may also be a quiet MXRB candidate (Boyajian et al. 2005), which we observed to refine its orbital elements. We measured V_r for HD 15137 using the same Balmer, He I, and He II lines we used for HD 14633. Because of the broad lines in the spectrum of HD 15137, we find significantly more scatter than in the case of HD 14633. Our V_r measurements are listed in Table 4.

For HD 15137, we collected 34 published V_r measurements from Conti et al. (1977) and Boyajian et al. (2005) to include with our 14 new measurements. A period search using this complete data set suggests a period of 30.35 days, slightly higher than our preliminary result (28.61 days; Boyajian et al. 2005). The addition of our new measurements also affects the other orbital elements, and our revised orbital solution is presented in Table 3. However, we stress that the period of HD 15137 relies heavily on the single observation from Conti et al. (1977), and thus, it remains highly uncertain. Better orbital coverage will improve the results significantly.

3.4. Feige 25

On five of the seven nights we observed Feige 25, we obtained two 30 minute exposures, which we co-added for better S/N. On the remaining nights, we were only able to obtain a single 30 minute exposure. The high- σ in our measurements likely results from the low-S/N in our spectra, since the noisy He I and Mg II lines were difficult to fit. While we observe some scatter in the V_r set, it is not significant, and the velocity remains constant within the measured errors. Since our measurements are also consistent with the values $V_r = 24.1 \pm 12.1$ (Martin 2006) and $V_r = -5 \pm 25$ (Greenstein & Sargent 1974), we classify this star as radial velocity constant.

3.5. HD 30614

HD 30614 has been classified as an SB1 by Zejnalov & Musaev (1986), who found a 3.68 day period and highly eccentric ($e = 0.45$) orbit with a very low velocity semiamplitude, $K = 9 \text{ km s}^{-1}$. Such a low K would imply a very low inclination in a massive SB1, and selection effects make it extremely difficult to detect such systems. We combined our 15 observations with additional measurements of its V_r from Beardsley (1969), Conti et al. (1977), Bohannon & Garmany (1978), Stone (1982), Gies & Bolton (1986), and Zejnalov & Musaev (1986). A new period search using this complete data set revealed the possible $P = 3.24$ days. However, these studies each used the mean V_r from many lines, and the interline scatter is comparable to the low K found by Zejnalov & Musaev (1986).

Instead of using all of these data, we chose to investigate a small subset of lines with the hope of reducing the scatter in the radial velocity curve. Only Zejnalov & Musaev (1986) and D. R. Gies (2006, private communication) provided V_r measurements for individual lines, and three lines are common to our data sets: Si IV $\lambda\lambda 4089, 4116$ and H δ . Since HD 30614 is a nonradial pulsator with variable stellar winds (Fullerton et al. 1996; Rzaev & Panchuk 2004), the Balmer lines may be contaminated. Therefore, we chose to use the mean from only the two Si IV lines, which usually agree within 4 km s^{-1} in our data. We repeated the period search using this subset of data, and we found a strong signal at $P = 3.57$ days, closer to that found by Zejnalov & Musaev (1986), but the low-amplitude variations probably originate in atmospheric or wind modulations rather than orbital motion. Without the availability of higher resolution spectra, we conclude that HD 30614 is more likely a single star that has been misclassified.

3.6. HD 36576

Because the H Balmer lines have strong emission in this B2 IV–Ve star, we used only the available He I lines to measure V_r , listed in Table 5. Even among these lines, their asymmetric profiles caused some difficulty in our measurements, resulting in a large scatter for each V_r . The 2AOV test confirms that the high- σ is due to our measurement errors rather than real velocity differences between lines. In our sequence of observations, we find rapid yet low-amplitude variations in V_r that suggest that non-radial pulsations may be present in this star.

3.7. HD 37737

An orbital solution for HD 37737 was originally published by Gies & Bolton (1986) with an orbital period of 2.49 days. However, our period search using our data with theirs resulted in a very different period of 7.84 days. Even using only Gies & Bolton's data, we found the same period with the modern CLEAN algorithm. We conclude that the original period was in error, and we present new orbital elements for this SB1 in Table 3. Figure 1 shows that the Gies & Bolton (1986) data agree well with our data and the new orbital solution.

3.8. HD 52266

We measured V_r for HD 52266, listed in Table 5, using the mean from many H Balmer, He I, and He II lines. The star has very broad lines that contribute to the high scatter in our measurements, and the short-term changes in V_r are usually smaller than the measured errors. However, we find a definite increase in V_r between the October and November runs that is statistically significant in our 2AOV test. We suspect that HD 52266 may be a SB1 with a period too long to measure from our data.

3.9. HD 52533

We initially measured V_r for HD 52533 using many H Balmer, He I, and He II lines. The mean velocity from the Balmer lines varies from 3 to 122 km s^{-1} , and comparable variations are seen in the He I lines. However, the He II line measurements have a much higher amplitude of variation, from -18 to 206 km s^{-1} ! These lines indicate significant LL variations in this star, and the 2AOV test reveals that the probability of these variations originating from random fluctuations within the same sample is negligible. We suspect that this may be a triple star system; the He II line probably originates in the hottest component, an O-type primary star in a close spectroscopic binary. A cooler, B-type companion is probably a widely separated, stationary star. Its strong He I and Balmer lines cause blending in these line profiles without affecting the He II lines. HD 52533 is not a known speckle binary. Most recently, it was observed but not resolved by B. Mason in 2006 November (private communication), placing an upper limit of 30 mas on the angular separation of the wide components assuming $\delta V < 3$.

Because of the suspected line blending, we investigate the orbit of the primary using the mean V_r from only the He II $\lambda\lambda 4200, 4542, \text{ and } 4686$ lines. D. R. Gies (2006, private communication) provided 10 measurements of these lines that we combine with our 20 observations to determine the primary's orbital period, $P = 22.19$ days. Only one He II line was recorded in our coude feed spectra, and the large scatter in Gies's data led us to use only one or two of his He II line measurements in some cases. For each V_r based on only one line instead of a mean, we assigned the point only half-weight. The resulting orbit of the primary is presented in Table 3, and its V_r measurements are listed in Table 4. We will explore this system in more detail in a forthcoming paper.

TABLE 6
STELLAR PHYSICAL PARAMETERS

Star (1)	Spectral Type (2)	T_{eff} (K) (3)	$\log g$ (4)	$v \sin i$ (km s ⁻¹) (5)	$E(B-V)$ (6)	R (7)	θ_{LD} (μ as) (8)	d (pc) (9)	Derived R_* (R_{\odot}) (10)	Expected R_* (R_{\odot}) (11)	Adopted d (pc) (12)	References (13)
HD 1976	B5 IV	16100	3.8	160	0.13 \pm 0.02	2.60 \pm 0.5	184 \pm 9	190	3.8 \pm 0.2	5.7	240 \pm 50	1
HD 14633	O8.5 V	35100	3.95	138	0.13 \pm 0.02	3.18 \pm 0.5	40 \pm 2	2150	9.2 \pm 0.4	8.3	2040 \pm 110	2, 3
HD 15137	O9.5 V	29700	3.50	234	0.43 \pm 0.04	3.18 \pm 0.5	56 \pm 7	2650	16.1 \pm 1.9	13.2	2420 \pm 230	2, 3
Feige 25	B7	13200	4.0	250	0.12 \pm 0.01	2.94 \pm 0.1	11 \pm 0.1	2800	3.3 \pm 0.03	3.0	2670 \pm 130	1, 4
HD 30614	O9.5 Iac	29000	3.0	118	0.33 \pm 0.04	3.21 \pm 0.3	269 \pm 21	1200	34.7 \pm 2.7	36.8	1240 \pm 40	1, 5, 6
HD 36576	B2 IVe	26060	3.82	165	0.45 \pm 0.06	3.28 \pm 0.4	211 \pm 14	310	7.0 \pm 0.5	7.3	320 \pm 10	1, 7, 8
HD 37737	O9.5 III	29800	3.95	182	0.69 \pm 0.04	2.88 \pm 0.2	69 \pm 4	2300	17.1 \pm 0.9	7.2	1640 \pm 660	2, 9, 10
HD 52266	O9 V	31000	3.75	248	0.31 \pm 0.01	3.32 \pm 0.4	66 \pm 5	1700	12.0 \pm 0.9	13.4	1790 \pm 90	2, 6
HD 52533	O9 V	32400	3.95	270	0.21 \pm 0.03	3.17 \pm 0.5	42 \pm 1	2000	9.0 \pm 0.2	7.9	1880 \pm 120	2, 6
HD 60848	O8 V:pevar	31600	4.20	163	0.18 \pm 0.02	3.27 \pm 0.5	63 \pm 4	1900	12.8 \pm 0.8	7.2	1480 \pm 420	2, 6
HD 188001	O7.5 Ia	34080	3.36	94	0.32 \pm 0.05	3.18 \pm 0.2	99 \pm 5	3200	34.0 \pm 1.6	20.8	2580 \pm 620	2, 6
HD 195592	O9.5 Ia	30460	3.19	114	1.17 \pm 0.04	3.02 \pm 0.2	220 \pm 12	1400	33.1 \pm 1.8	22.1	1170 \pm 230	2, 6

REFERENCES.—(1) Schaller et al. 1992; (2) Martins et al. 2005; (3) van Steenberg & Shull 1988; (4) Martin 2006; (5) Crowther et al. 2006; (6) Mason et al. 1998; (7) Abt et al. 2002; (8) Chauville et al. 2001; (9) Leitherer 1988; (10) Patriarchi et al. 2003.

3.10. HD 60848

The H β , H γ , and He I λ 4713 lines in HD 60848 show double-peaked emission in our spectra; therefore, we omitted these lines in our V_r measurements. Like HD 36576, we found rapid, low-amplitude variations in V_r in HD 60848 that are consistent with nonradial pulsations, and we classify this star as single. The high scatter in our measurements is not statistically significant, and it is likely due to the pulsations' effect on line profiles in HD 60848.

3.11. HD 188001

There are a wealth of V_r measurements for HD 188001 in the literature, and several groups (Underhill & Matthews 1995; Aslanov et al. 1984; Aslanov & Barannikov 1992) have published orbital solutions for this spectroscopic binary with periods ranging from 32.5 to 78.74 days. Our new observations do not agree with any of the previous solutions, so we decided to undertake a new analysis of this star using the available data. Thus, we gathered 14 measurements of V_r from Plaskett (1924), 2 from Conti et al. (1977), 11 from Bohannon & Garmany (1978), 8 from Garmany et al. (1980), 16 from Stone (1982), 17 from Aslanov et al. (1984), 20 from Fullerton (1990), 9 from Underhill (1995), and 8 new values from this work (listed in Table 5).

This complete sample of 105 V_r values is an inhomogeneous collection of measurements relying on different line groups and different wavelength regions, but the measured lines are predominantly He I and He II with some metal lines also included. To retain the maximum consistency between these data sets, whenever the authors present V_r from more than one line or line group, we chose to use only He I and He II lines in absorption. These lines also provided the most reliable V_r in our own measurements; however, they are probably affected by the stellar winds. We observe the He II λ 4686 line in emission, and Fullerton (1990) noted a variable P Cygni absorption trough in the He I λ 5876 line profiles, whereas the C IV λ 5801, 5812 lines in Fullerton's sample are more likely photospheric. Certainly we are concerned by the need to rely on wind lines to investigate the orbital period of HD 188001, but in lieu of a more complete data set from purely photospheric lines, we are limited in our approach.

We performed a period search with these 105 values, eliminating spurious frequencies that suggest periods less than 10 days, since rapid V_r variations are not observed in HD 188001. The strongest signal suggests a period $P = 29.83$ days; however, the

sinusoidal variation appears to be due to the systematic differences between various data sets rather than true orbital motion. Therefore, we conclude that HD 188001 is actually a single star, possibly with variable winds that contaminate the He absorption lines and mimic the signature of a spectroscopic binary.

3.12. HD 195592

We did not use the H Balmer lines to measure V_r in HD 195592 due to their inverse P Cygni profiles, suggesting that wind emission is partially filling in these lines. Instead we used strong, unblended He I, He II, and Si IV lines to measure velocities. We find that V_r is slightly lower during our November run than in October, and the 2AOV statistical test indicates that this difference is highly significant. Therefore, we believe HD 195592 may be a SB1 system. We combined our data with eight V_r measurements from Mayer et al. (1994) to search for a possible orbital period, but the only significant signal occurred at the unphysical period ~ 0.5 days. Additional data is needed to determine if HD 195592 is indeed a binary.

4. SPECTROSCOPIC MODELING AND SED FITS

Our O- and B-type targets include a wide range of spectral types, luminosity types, and even emission stars, making it difficult to obtain the temperature and surface gravity of every star. Nonetheless, we used a combination of sources to obtain their physical parameters. The resulting values, and references where applicable, are listed in Table 6.

For the B-type stars HD 1976 and Feige 25, we generated a grid of synthetic, plane-parallel, local thermodynamic equilibrium (LTE) atmospheric models using the Kurucz ATLAS9 code (Kurucz 1994). We adopted solar abundances and a microturbulent velocity of 2 km s⁻¹ for these stars, which corresponds to the mean microturbulence observed among late-type, main-sequence B stars (Lyubimkov et al. 2004). Each atmospheric model was then used to calculate a grid of model spectra using SYNSPEC (Lanz & Hubeny 2003). Using the measured V_r from each observation, we shifted each observed spectrum to its rest frame and created a mean spectrum of each target to compare with the model grid. We compared the observed three H Balmer line profiles to model profiles convolved with a limb-darkened, rotational broadening function and a Gaussian instrumental broadening function to measure T_{eff} , $\log g$, and $v \sin i$. For each fit, we used steps of 100 K in T_{eff} , 0.1 dex in

$\log g$, and 10 km s^{-1} in $v \sin i$, and determined the best fit by minimizing the square of the residual, $(O-C)^2$, over a 40 \AA wide region centered on the rest wavelength of each line. The line wings are particularly sensitive to $\log g$, while the line depths are strong indicators of T_{eff} , since the strength of the Balmer lines declines steadily with increasing T_{eff} in the B spectral regime. Finally, the shape of the line core is most sensitive to $v \sin i$, so we were able to obtain excellent fits by adjusting these three parameters. Using this technique, we find errors of $\pm 100 \text{ K}$ in T_{eff} for Feige 25 and $\pm 400 \text{ K}$ for HD 1976. For both stars, the error in $\log g$ is ± 0.1 , and for $v \sin i$ it is $\pm 30 \text{ km s}^{-1}$. The resulting parameters for HD 1976 and Feige 25 are listed in columns (3)–(5) of Table 6. Our measurements of Feige 25 are in good agreement with the physical parameters found by Keenan & Dufton (1983) and Martin (2004).

For the hotter O-type stars, we used the OSTAR2002 grid of line-blanketed, non-LTE, plane-parallel, hydrostatic atmosphere model spectra for O-type stars from the TLUSTY code (Lanz & Hubeny 2003). These models adopt solar abundances and a fixed microturbulent velocity of 10 km s^{-1} . Once again, we convolved each model with a limb-darkened rotational broadening function and a Gaussian instrumental broadening function to compare with our observed spectra. Here we used step sizes of 100 K in T_{eff} , 0.05 in $\log g$, and 10 km s^{-1} in $v \sin i$. Because of the probable line blending in the Balmer and He I lines in HD 52533 and emission partially filling the He I line profiles in HD 60848, we used the $\text{He II } \lambda\lambda 4200, 4542, \text{ and } 4686$ lines to measure the physical parameters of each O-type dwarf. The resulting T_{eff} , $\log g$, and $v \sin i$ from the O star fits are listed in Table 6. Our measurement errors are typically 400 K in T_{eff} , 0.10 in $\log g$, and 10 km s^{-1} in $v \sin i$.

The Be star HD 36576 had obvious emission in its Balmer lines, and the O supergiants HD 30614, HD 188001, and HD 195592 were also difficult to fit with the plane-parallel spectral models. Therefore, we adopted T_{eff} and $\log g$ of HD 30614 and HD 36576 from Crowther et al. (2006) and Chauville et al. (2001), respectively. In addition, we adopted $v \sin i = 165 \text{ km s}^{-1}$ for HD 36576 (Abt et al. 2002). We used the spectral types of HD 188001 and HD 195592 to obtain their parameters from the calibration of Martins et al. (2005).

We then compared the resulting model spectrum to the observed spectral energy distribution (SED). For all of our targets except Feige 25 and HD 52533, flux-calibrated UV spectra were available from the *International Ultraviolet Explorer* (IUE) archives. We also obtained UV fluxes in several bandpasses from Thompson et al. (1978) and/or Wesselius et al. (1982) in most cases. For HD 52266 and HD 195592, the available IUE fluxes disagree with the other UV fluxes, so we prefer the UV bandpass photometry, which provides a continuous SED when combined with optical data. Johnson *UBVR* (from numerous sources in the VizieR database; Ochsenbein et al. 2000), Strömberg *uvby* (Hauck & Mermilliod 1998), and 2MASS *JHK* (Cutri et al. 2003) photometry were usually available as well. For these three filter systems, we converted the photometric magnitudes to fluxes using the techniques of Colina et al. (1996), Gray (1998), and Cohen et al. (2003), respectively. The model spectra were binned into 50 \AA bins in order to remove small-scale line structure and compare to the observed SED. For those stars with close binary or speckle companions that contribute to the SED, we neglect the companion's flux contribution in the model.

Using a grid of values for the reddening, $E(B-V)$, and the ratio of total-to-selective extinction, R , we compared the reddened absolute fluxes from the spectral models to the observed stellar flux. We used a step size of 0.01 for both parameters, and we determined the best-fit values of $E(B-V)$ and R by minimizing

$(O-C)^2$, and the typical errors are 0.03 and 0.4 mag , respectively. The ratio of the observed stellar flux to the reddened model flux provides the angular diameter, θ_{LD} , of each star (Gray 1992). The errors in θ_{LD} are determined from the standard deviation of the ratios from each optical and infrared flux estimate, since the ratio is wavelength independent. These measured parameters are listed in columns (6)–(8) of Table 6.

Distances to most of our targets were obtained from van Steenberg & Shull (1988), Mason et al. (1998), Patriarchi et al. (2003), and Martin (2006). For the remaining stars HD 1976 and HD 36576 we obtained an estimate of their absolute magnitudes from Wegner (2000) and combined these with the observed V and our calculated $A(V) = R \times E(B-V)$ to determine their distances. Finally, we used θ_{LD} with the known distances to determine the radius, R_* , for each star (col. [9] of Table 6). We note that the closest stars in our list, HD 1976 and HD 36576, also have *Hipparcos* parallaxes available, but the larger distances from these measurements (420 and 570 pc , respectively) imply significantly larger R_* than we expect for these stars.

In Table 6 we also provide the predicted R_* from the calibration of Martins et al. (2005) for stars with $T_{\text{eff}} > 30,000$, and for cooler stars we use the evolutionary models of Schaller et al. (1992) to determine the expected value. The observed differences between the derived and predicted radii are usually small, and we find no systematic differences between the binaries' and single stars' radii that may be due to neglecting the companion fluxes in the SED fits. Note that we do find large discrepancies in R_* for the binaries HD 37737 and HD 195592, but we also find a similar error for the single star HD 188001. All three stars are giants and supergiants, and the errors in their predicted physical parameters are larger (Martins et al. 2005). In these cases the distances require a significant downward revision to match our derived radii with the expected values. Therefore, we derive a new distance to each target based on the expected R_* and our measured θ_{LD} , and we adopt the mean of these two distances with errors representing the range of possible values. The final adopted distances are listed in Table 6.

We also inspected the observed SED to look for an IR excess in our targets, which may be indicative of an accretion disk around a compact companion. The emission-line stars HD 36576 and HD 60848 appear to have a small K-band flux excess due to their circumstellar disks, but no other targets show evidence of an IR excess.

5. RUNAWAY STATUS OF TARGETS

Our new radial velocity data and the distance constraints above allow us to reexamine the runaway status of each of our targets. We list in Table 7 (cols. [2] and [3]) the Galactic longitude, l , and latitude, b , for each star. Columns (4) and (5) give the proper motions, $\mu_\alpha \cos \delta$ and μ_δ , obtained from the Second US Naval Observatory CCD Astrograph Catalog (UCAC2; Zacharias et al. 2004) and the *UCAC2 Bright Star Supplement* (Urban et al. 2004). We computed the peculiar transverse and radial space velocity, $V_{t,\text{pec}}$ and $V_{r,\text{pec}}$, of each star using the method of Berger & Gies (2001), and these are listed in columns (6) and (7). These are combined into a single measure of the peculiar space velocity, V_{pec} , in column (8). Our values of $V_{t,\text{pec}}$ and $V_{r,\text{pec}}$ for HD 37737 and HD 52533 agree closely with those found by Moffat et al. (1998).

We classify as definite runaways those stars with $V_{\text{pec}} > 30 \text{ km s}^{-1}$ plus the error in V_{pec} (Gies & Bolton 1986), and we find seven such stars among our sample: HD 14633, HD 15137, Feige 25, HD 30614, HD 36576, HD 188001, and HD 195592. Our findings agree with those of Noriega-Crespo et al. (1997), who found bow shocks associated with HD 30614, HD 188001,

TABLE 7
PECULIAR SPACE VELOCITIES

Star (1)	l (deg) (2)	b (deg) (3)	$\mu_{\alpha}\cos\delta$ (mas yr ⁻¹) (4)	μ_{δ} (mas yr ⁻¹) (5)	$V_{l,pec}$ (km s ⁻¹) (6)	$V_{r,pec}$ (km s ⁻¹) (7)	V_{pec} (km s ⁻¹) (8)
HD 1976	118.68	-10.63	13.70 ± 0.25	-4.40 ± 0.42	4.8 ± 1.4	-9.2 ± 0.8	10.4 ± 1.6
HD 14633	140.78	-18.20	-0.4 ± 0.7	-7.8 ± 1.0	66.6 ± 12.4	-24.1 ± 1.7	70.8 ± 12.5
HD 15137	137.46	-7.58	0.67 ± 0.40	-5.08 ± 0.73	57.0 ± 11.0	-26.2 ± 4.2	62.7 ± 11.8
Feige 25	165.42	-48.36	4.4 ± 1.1	-0.3 ± 1.2	58.7 ± 21.8	33.2 ± 4.3	67.4 ± 22.2
HD 30614	144.07	+14.04	0.49 ± 0.18	7.31 ± 0.45	46.9 ± 3.2	21.9 ± 2.7	51.8 ± 4.2
HD 36576	187.39	-7.84	0.15 ± 1.20	0.01 ± 0.48	6.8 ± 1.9	34.1 ± 3.3	34.7 ± 3.8
HD 37737	173.46	+3.24	0.8 ± 0.6	-4.2 ± 0.6	25.5 ± 13.9	-12.9 ± 3.1	28.6 ± 14.3
HD 52266	219.13	-0.68	-0.89 ± 0.78	-0.70 ± 0.61	18.9 ± 8.5	-4.5 ± 3.1	19.4 ± 9.0
HD 52533	216.85	+0.80	-0.67 ± 2.54	-0.04 ± 1.81	13.2 ± 27.8	45.1 ± 2.0	47.0 ± 27.9
HD 60848	202.51	+17.52	-3.43 ± 0.75	-1.41 ± 0.50	12.7 ± 7.4	2.2 ± 5.7	12.9 ± 9.4
HD 188001	56.48	-4.33	-0.17 ± 0.48	-10.45 ± 0.34	81.5 ± 22.0	-2.3 ± 4.3	81.5 ± 22.4
HD 195592	82.36	+2.96	-2.46 ± 0.48	1.62 ± 0.51	37.2 ± 7.9	-20.1 ± 2.1	42.3 ± 8.2

and HD 195592 due to their fast space velocities. Uncertainties in the proper motions and distances contribute to large errors in V_{pec} for several of our stars, so the tentative runaways HD 37737 and HD 52533 also have $V_{pec} > 30$ km s⁻¹ within their errors. Having a lower V_{pec} does not exclude the possibility that a star was ejected in the past—as long as its velocity is greater than the escape velocity from the cluster, an ejected star will effectively be a runaway.

Although we find that HD 37737 is tentatively a runaway, it is worthwhile to note that the star has also been classified as a member of the Aur OB1 association (Humphreys 1978). It may also be surrounded by a symmetric H II bubble (Noriega-Crespo et al. 1997), although the morphology of the bubble is difficult to classify with certainty. To investigate whether HD 37737 is a member of Aur OB1, we compared its proper motion to those of the other proposed Aur OB1 members using the UCAC2 and *UCAC2 Bright Star Supplement* catalogs. We find that HD 37737 and seven other stars from Humphrey's list do indeed have similar proper motions, although the remaining seven stars are moving in nearly an opposite direction. From these results we doubt that the Aur OB1 association is truly a bound group, but the evidence does suggest that multiple open clusters may be superimposed on this region of the sky. Further investigation of the groups' distances are required to determine whether HD 37737 is a member.

The stars HD 1976, HD 52266, and HD 60848 have low V_{pec} and are probably not runaway stars. HD 52266 (along with the higher velocity systems HD 52533 and HD 195592; de Wit et al. 2004) may be a member of a previously undetected cluster. Since our spectra of HD 52533 suggest that it may be a triple system, it is very likely that a sparse cluster indeed exists and that this system is not a runaway. We will explore this possibility in the future.

Our search was designed to detect runaway binary systems, and it is no surprise that we identify several in our sample (HD 14633, HD 15137, HD 195592, and the possible runaway HD 37737). Both dynamical interactions within a dense open cluster and a supernova in a close binary can produce runaway SB1 systems, and our results highlight how rare such systems are. These ejection mechanisms can be distinguished observationally, and we will explore both scenarios for HD 14633 and HD 15137 in a forthcoming paper.

We thank the referee for his/her careful consideration of this work. We are grateful to Di Harmer for her assistance at the telescope, and we also thank John Martin and Alex Fullerton for providing their thesis data and for their helpful comments on this work. Kathy Vieira, Bill van Altena, and Norbert Zacharias contributed useful advice about the proper-motion analysis. This material is based on work supported by the National Science Foundation under grants AST 02-05297, AST 04-01460, and AST 05-06573. Institutional support has been provided from the Georgia State University (GSU) College of Arts and Sciences and from the Research Program Enhancement fund of the Board of Regents of the University System of Georgia, administered through the GSU Office of the Vice President for Research. Some of the data presented in this paper were obtained from the Multimission Archive at the Space Telescope Science Institute (MAST). STScI is operated by the Association of Universities for Research in Astronomy, Inc., under NASA contract NAS5-26555. Support for MAST for non-*HST* data is provided by the NASA Office of Space Science via grant NAG5-7584 and by other grants and contracts.

Facilities: KPNO:2.1m, IUE (SWP, LWP, LWR)

REFERENCES

- Abt, H. A., Gomez, A. E., & Levy, S. G. 1990, *ApJS*, 74, 551
 Abt, H. A., Levato, H., & Grosso, M. 2002, *ApJ*, 573, 359
 Allen, C., Poveda, A., & Hernández-Alcántara, A. 2006, *Rev. Mex. AA Ser. Conf.*, 25, 13
 Aslanov, A. A., & Barannikov, A. A. 1992, *Soviet Astron. Lett.*, 18, 58
 Aslanov, A. A., Kornilova, L. N., & Cherepashchuk, A. M. 1984, *Soviet Astron. Lett.*, 10, 278
 Bally, J., & Zinnecker, H. 2005, *AJ*, 129, 2281
 Beardsley, W. R. 1969, *Publ. Allegheny Obs.*, 8, 91
 Berger, D. H., & Gies, D. R. 2001, *ApJ*, 555, 364
 Blaauw, A. 1961, *Bull. Astron. Inst. Netherlands*, 15, 265
 Blaauw, A., & van Albada, T. S. 1963, *ApJ*, 137, 791
 Bohannon, B., & Garmany, C. D. 1978, *ApJ*, 223, 908
 Bolton, C. T., & Rogers, G. L. 1978, *ApJ*, 222, 234
 Boyajian, T. S., Beaulieu, T. D., Gies, D. R., Huang, W., McSwain, M. V., Riddle, R. L., Wingert, D. W., & De Becker, M. 2005, *ApJ*, 621, 978
 Casares, J., Ribó, M., Ribas, I., Paredes, J. M., Martí, J., & Herrero, A. 2005, *MNRAS*, 364, 899
 Chauville, J., Zorec, J., Ballereau, D., Morrell, N., Cidale, L., & Garcia, A. 2001, *A&A*, 378, 861
 Cohen, M., Wheaton, W. A., & Megeath, S. T. 2003, *AJ*, 126, 1090
 Colina, L., Bohlin, R. C., & Castelli, F. 1996, *Hubble Space Telescope Instrument Science Rep. CAL/SCS-008* (Baltimore: STScI)
 Conti, P. S., Leep, E. M., & Lorre, J. J. 1977, *ApJ*, 214, 759
 Crowther, P. A., Lennon, D. J., & Walborn, N. R. 2006, *A&A*, 446, 279
 Cutri, R. M., et al. 2003, *The 2MASS All-Sky Catalog of Point Sources* (Pasadena: IPAC)
 de Wit, W. J., Testi, L., Palla, F., Vanzì, L., & Zinnecker, H. 2004, *A&A*, 425, 937

- De Zeeuw, P. T., Hoogerwerf, R., De Bruijne, J. H. J., Brown, A. G. A., & Blaauw, A. 1999, *AJ*, 117, 354
- Docobo, J. A., & Costa, J. M. 1986, *ApJS*, 60, 945
- Dray, L. M., Dale, J. E., Beer, M. E., Napiwotzki, R., & King, A. R. 2005, *MNRAS*, 364, 59
- Fullerton, A. W. 1990, Ph.D. thesis, Univ. Toronto
- Fullerton, A. W., Gies, D. R., & Bolton, C. T. 1996, *ApJS*, 103, 475
- Garmany, C. D., Conti, P. S., & Massey, P. 1980, *ApJ*, 242, 1063
- Gies, D. R., & Bolton, C. T. 1986, *ApJS*, 61, 419
- Gray, D. F. 1992, *The Observation and Analysis of Stellar Photospheres* (2nd ed.; Cambridge: Cambridge Univ. Press)
- Gray, R. O. 1998, *AJ*, 116, 482
- Greenstein, J. L., & Sargent, A. I. 1974, *ApJS*, 28, 157
- Gualandris, A., Portegies Zwart, S., & Eggleton, P. P. 2004, *MNRAS*, 350, 615
- Hartkopf, W. I., et al. 2000, *AJ*, 119, 3084
- Hauck, B., & Mermilliod, M. 1998, *A&AS*, 129, 431
- Hoogerwerf, R., de Bruijne, J. H. J., & de Zeeuw, P. T. 2001, *A&A*, 365, 49
- Humphreys, R. M. 1978, *ApJS*, 38, 309
- Keenan, F. P., & Dufton, P. L. 1983, *MNRAS*, 205, 435
- Kurucz, R. L. 1994, CD-ROM 19, *Solar Abundance Model Atmospheres for 0, 1, 2, 4, 8 km/s* (Cambridge: SAO)
- Lanz, T., & Hubeny, I. 2003, *ApJS*, 146, 417
- Leitherer, C. 1988, *ApJ*, 326, 356
- Leonard, P. J. T., & Duncan, M. J. 1990, *AJ*, 99, 608
- Lyubimkov, L. S., Rostopchin, S. I., & Lambert, D. L. 2004, *MNRAS*, 351, 745
- Martin, J. C. 2004, *AJ*, 128, 2474
- . 2006, *AJ*, 131, 3047
- Martins, F., Schaerer, D., & Hillier, D. J. 2005, *A&A*, 436, 1049
- Mason, B. D., Gies, D. R., Hartkopf, W. I., Bagnuolo, W. G., ten Brummelaar, T., & McAlister, H. A. 1998, *AJ*, 115, 821
- Mason, B. D., Wycoff, G. L., Hartkopf, W. I., Douglass, G. G., & Worley, C. E. 2001, *AJ*, 122, 3466
- Mathias, P., Aerts, C., Briquet, M., De Cat, P., Cuypers, J., Van Winckel, H., & Le Contel, J. M. 2001, *A&A*, 379, 905
- Mayer, P., Chochol, D. C., Hanna, M. A.-M., & Wolf, M. 1994, *Contrib. Astron. Obs. Skalnaté Pleso*, 24, 65
- McSwain, M. V., & Gies, D. R. 2005, *ApJS*, 161, 118
- McSwain, M. V., Gies, D. R., Huang, W., Wiita, P. J., Wingert, D. W., & Kaper, L. 2004, *ApJ*, 600, 927
- Meurs, E. J. A., Fennell, G., & Norci, L. 2005, *ApJ*, 624, 307
- Moffat, A. F. J., et al. 1998, *A&A*, 331, 949
- Morbey, C. L., & Brosterhus, E. B. 1974, *PASP*, 86, 455
- Motch, C., et al. 1998, *A&AS*, 132, 341
- Noriega-Crespo, A., van Buren, D., & Dgani, R. 1997, *AJ*, 113, 780
- Ochsenbein, F., Bauer, P., & Marcout, J. 2000, *A&AS*, 143, 23
- Patriarchi, P., Morbidelli, L., & Perinotto, M. 2003, *A&A*, 410, 905
- Philp, C. J., Evans, C. R., Leonard, P. J. T., & Frail, D. A. 1996, *AJ*, 111, 1220
- Plaskett, J. S. 1924, *Publ. Dom. Astrophys. Obs. Victoria*, 2, 285
- Portegies Zwart, S. F. 2000, *ApJ*, 544, 437
- Poveda, A., Ruiz, J., & Allen, C. 1967, *Bol. Obs. Tonantzintla Tacubaya*, 4, 86
- Ribó, M., Paredes, J. M., Romero, G. E., Benaglia, P., Martí, J., Fors, O., & García-Sánchez, J. 2002, *A&A*, 384, 954
- Roberts, D. H., Lehar, J., & Dreher, J. W. 1987, *AJ*, 93, 968
- Rzayev, A. K., & Panchuk, V. E. 2004, *Astron. Lett.*, 30, 332
- Sayer, R. W., Nice, D. J., & Kaspi, V. M. 1996, *ApJ*, 461, 357
- Schaller, G., Schaerer, D., Meynet, G., & Maeder, A. 1992, *A&AS*, 96, 269
- Stickland, D. J., & Lloyd, C. 2001, *Observatory*, 121, 1
- Stone, R. C. 1982, *ApJ*, 261, 208
- Thompson, G. I., Nandy, K., Jamar, C., Monfils, A., Houziaux, L., Carnochan, D. J., & Wilson, R. 1978, *Catalogue of Stellar Ultraviolet Fluxes* (London: Sci. Res. Council)
- Underhill, A. B. 1995, *ApJS*, 100, 433
- Underhill, A. B., & Matthews, J. M. 1995, *PASP*, 107, 513
- Urban, S. E., Zacharias, N., & Wycoff, G. L. 2004, *The UCAC2 Bright Star Supplement* (Washington: US Naval Obs.)
- van Steenberg, M. E., & Shull, J. M. 1988, *ApJS*, 67, 225
- Voges, W., et al. 2000, *IAU Circ.*, 7432, 1
- Wegner, W. 2000, *MNRAS*, 319, 771
- Wesselius, P. R., van Duinen, R. J., de Jonge, A. R. W., Aalders, J. W. G., Luinge, W., & Wildeman, K. J. 1982, *A&AS*, 49, 427
- Zacharias, N., Urban, S. E., Zacharias, M. I., Wycoff, G. L., Hall, D. M., Monet, D. G., & Rafferty, T. J. 2004, *AJ*, 127, 3043
- Zejnalo, S. K., & Musaev, F. A. 1986, *AZh Pis'ma*, 12, 304
- Zorec, J., Frémat, Y., & Cidale, L. 2005, *A&A*, 441, 235
- Zwicky, F. 1957, *Morphological Astronomy* (Berlin: Springer)